LASER INTERFEROMETER GRAVITATIONAL WAVE OBSERVATORY
- LIGO -
CALIFORNIA INSTITUTE OF TECHNOLOGY
MASSACHUSETTS INSTITUTE OF TECHNOLOGY

LIGO-xxxxxxx-xx-x 2012/04/23

GEO Squeezing Noise Budget

Kate Dooley, Hartmut Grote, Henning Vahlbruch (*alphabetical order for now*)

Distribution of this document:

LIGO Scientific Collaboration

Draft

California Institute of Technology
LIGO Project, MS 18-34
Pasadena, CA 91125
Phone (626) 395-2129
Fax (626) 304-9834
E-mail: info@ligo.caltech.edu

Massachusetts Institute of Technology
LIGO Project, Room NW17-161
Cambridge, MA 02139
Phone (617) 253-4824
Fax (617) 253-7014
E-mail: info@ligo.mit.edu

LIGO Hanford Observatory
Route 10, Mile Marker 2
Richland, WA 99352
Phone (509) 372-8106
Fax (509) 372-8137
E-mail: info@ligo.caltech.edu

LIGO Livingston Observatory
19100 LIGO Lane
Livingston, LA 70754
Phone (225) 686-3100
Fax (225) 686-7189
E-mail: info@ligo.caltech.edu

http://www.ligo.caltech.edu/

Table 1: OMC parameters. Many numbers come from p.12 of the GEO-HF logbook.

quantity	symbol	value	units
Finesse	F	160	
round trip length	L	0.658	m
g-factor	g	0.735	
waist size	ω_0	450	µm
free spectral range	FSR	455.6	MHz
Michelson sideband power transmission	T_{MI}	1.01	%
SRC sideband power transmission	T_{SR}	2.71	%

1 Introduction

2 Overview of squeezing setup

squeezer coherent control sidebands, Faraday isolator injection point, ...

Table 1 summarizes the current output mode cleaner (OMC) design parameters. Note that the sideband transmission numbers (T_{MI} and T_{SR}) should be doubled in practice to account for the existence of both upper and lower sidebands.

3 Reductions to potential squeezing

The amount of squeezing that can be achieved with an interferometer is a function of three things:

1. level of injected squeezing
2. optical losses (including mode-matching and alignment)
3. phase noise

3.1 Injected squeezing

The level of injected squeezing is of course limited to the performance of the squeezer itself. The level of squeezing generated by the squeezer can be controlled during interferometer operations by changing the setpoint for the Mach-Zehnder (MZ) in the squeezing box. A PZT on one of the MZ mirrors changes the MZ length and therefore controls the amount of green light transmitted through the MZ to match the requested setpoint. This green light

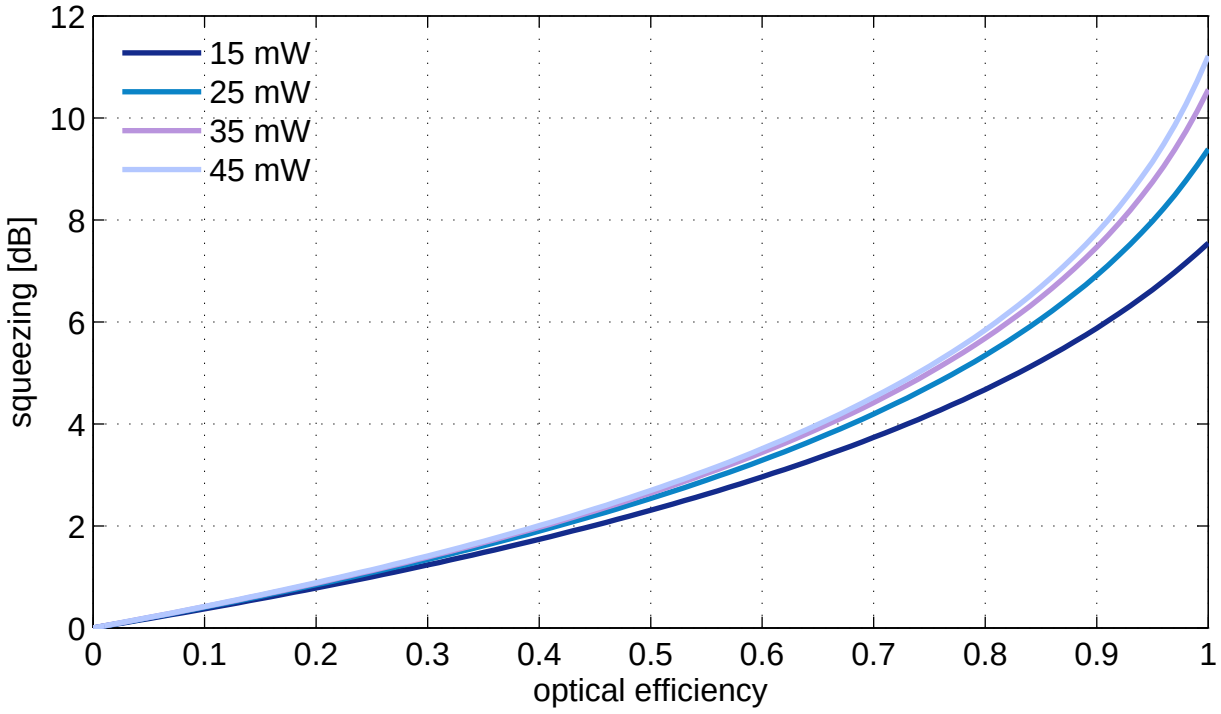

Figure 1: The expected amount of observed squeezing based on the green pump power and the optical efficiency of the squeezed beam path. This model assumes no phase noise.

(the pump field) is sent directly into the OPA cavity to generate the correlated 1064 nm photons. The degree of squeezing is a non-linear function of the pump power.

A maximum pump power of 45 mW, or 11 dB of generated squeezing, may be used with the GEO squeezer. However, in finding a balance between the benefits of more squeezing and the disadvantages of anti-squeezing (due to phase noise), the practical upper-limit on pump power was placed at 35 mW, or 10.5 dB of generated squeezing [Ref. Khalaidovski thesis]. (We should re-evaluate this limit.)

3.2 Optical losses

Any time the squeezed vacuum field experiences an optical loss, the loss is replaced by the classic vacuum field:

$$V' = VT - L \tag{1}$$

Here, V is the initial variance of the squeezed state, T the optical efficiency, and L the optical losses, where $T + L = 1$. Figure 1 shows the how the degree of squeezing is degraded as a function of optical efficiency for several different pump powers.

Table 2: Optical losses of squeezed beam. The resulting transmission upon multiplying the optical efficiencies in series is 63%.

component	power loss	comment
squeezer path Faraday	3.3%	1.5%
output port Faraday	3.3% × 2	guess
BDO1 transmission	1% × 2	
SR cavity (when locked)	1%	above 1 kHz
OMC mode-matching loss	6%	
squeezer mode-matching loss	2%	
OMC AR coating loss	1%	
OMC internal losses	14%	deduced from other measurements
OMC trans PD detection loss	9%	Perkin-Elmer

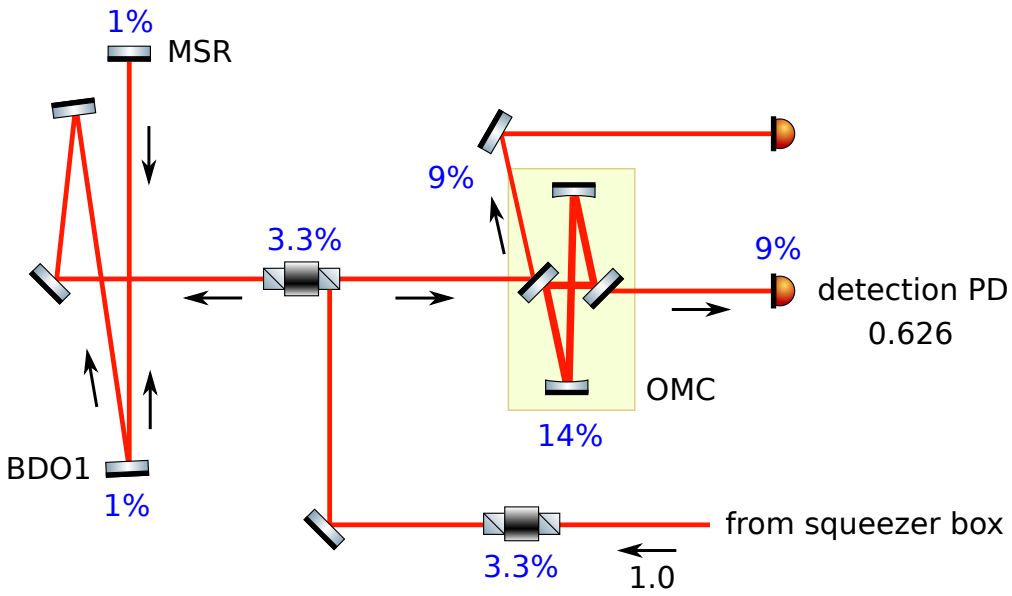

Figure 2: Optical losses in the squeezer path.

3.3 Phase noise

4 Optical losses

Table 2 summarizes our optical loss budget for the squeezer path. We find that only 63% of the squeezed light sent into the interferometer makes it to the detection PD. With the nominal 35 mW pump power, or 10.5 dB injected squeezing, these optical losses alone reduce the maximum possible level of achieved squeezing to 3.7 dB.

The single greatest source of loss is the OMC and second is the detection PD. The OMC is known to have excessive losses due to poor AR coatings and most likely dirty mirrors and can in principle be easily improved with new optics. The current Perkin-Elmer photodiode

is also a high-loss component that can be replaced with a much better specimen. The polarizing beam splitters of the Faraday isolators each have approximately 1% loss and with investigation into better polarizers, may be improved. Details of short-term goals for improvement of optical efficiency are found in Section 8.

5 Phase noise

The squeezing ellipse orientation must match the angle of the interferometer output field to make the best use of the squeezed field. The interferometer output field is ideally made up of only the local oscillator for the gravitational-wave signal, the dark fringe offset. However, in practice, other light is present and contributes to the shot noise at the detector. The power of squeezing is that it can reduce the shot noise of the light at the output port, no matter what it is made of. Therefore, the sum of the phase jitters of all fields must be considered. In addition, it should be pointed out that only the rms phase noise matters, not the shape of the frequency content.

5.1 Phase noise sensing and control

There are several options for how to implement a squeezer longitudinal phase servo. First, there are three choices for how to generate such an error signal. ...

Second, there are choices for how to feedback a control signal. ...

Our current setup for creating a squeezer to GEO output relative phase error signal uses the beat of the squeezer sidebands with the Michelson sidebands in reflection of the OMC which are at 15.2 MHz and 14.9 MHz, respectively. A sample error point spectrum is shown in Figure 3 and demonstrates that we measure only 5 mrad rms residual phase noise. We also inject a line at 6500 Hz to monitor the signal-to-noise of the error signal.

5.2 Noiselock

We implement a slow servo called the *noiselock loop* that serves to change the squeezing quadrature in order to maximize the strain sensitivity. The demodulation phase of the longitudinal phase error signal is dithered at 11.6 Hz and a band-limited root-mean-square of strain is then demodulated at this dither frequency and a control signal derived. A schematic of the servo is in Figure 4. The underlying causes for slow phase drift is not understood at this time. An example of how much drift we observe is shown in Figure 5.

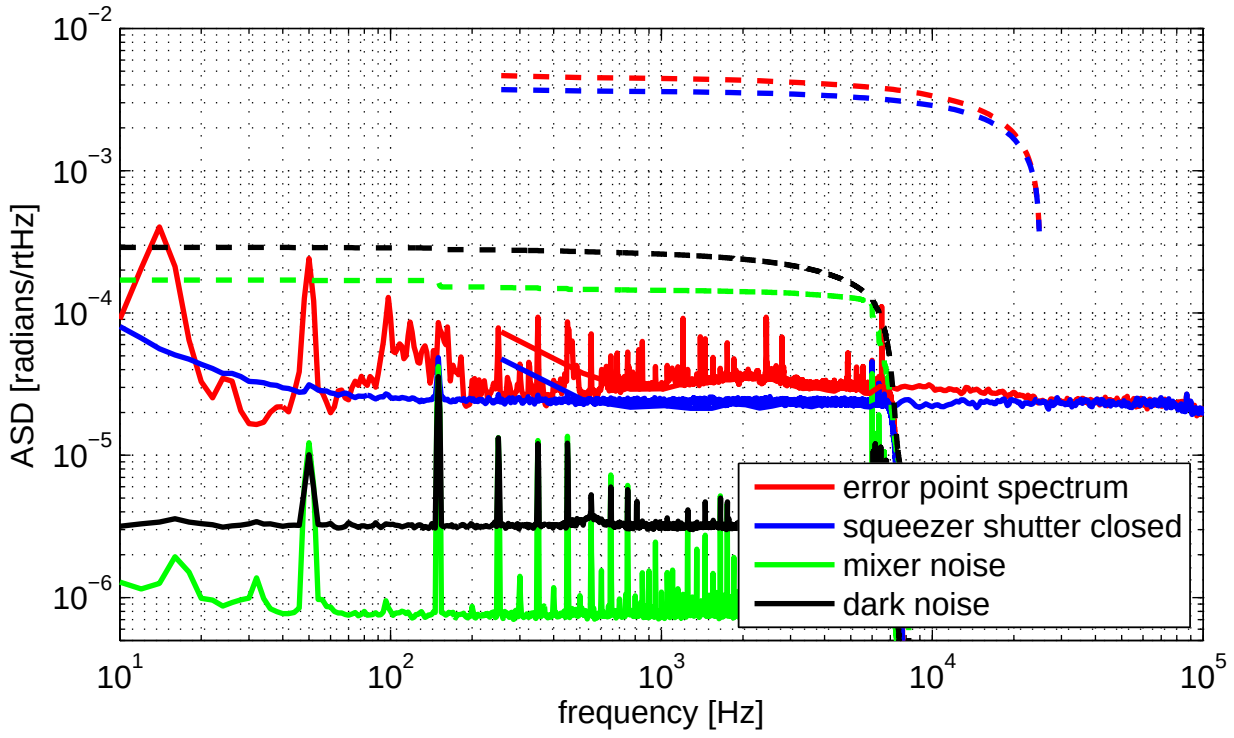

Figure 3: Calibrated squeezer phase error point (red curve), measured as the beat between the squeezer control sidebands and the RF Michelson sidebands in reflection of the OMC. This loop operates with a bandwidth of about 1 kHz and is limited by sensor/shot (blue curve) above 25 kHz. The servo is not gain-limited because the spectrum is so flat such that little to no improvement in rms noise is to be gained by increasing the gain. The residual rms phase noise is 5 mrad.

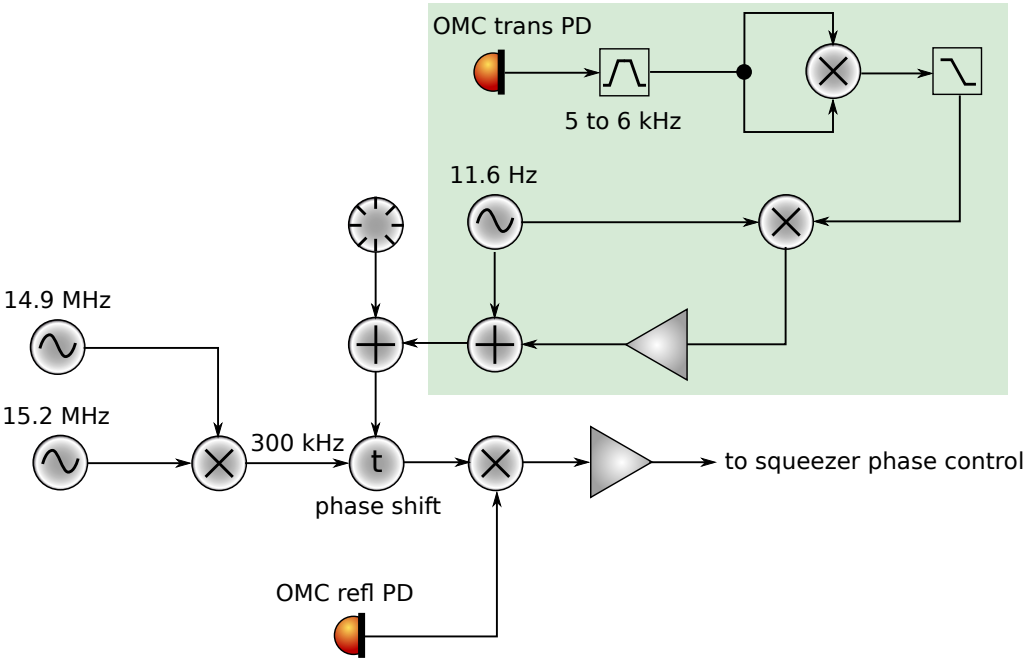

Figure 4: Schematic of the noiselock servo. The demodulation phase of the squeezing angle error signal is modulated at $f_0 = 11.6$ Hz. The band-limited rms of interferometer strain is in turn demodulated at f_0 and a derived control signal is in turn sent to the demodulation phase of the squeezing angle error signal.

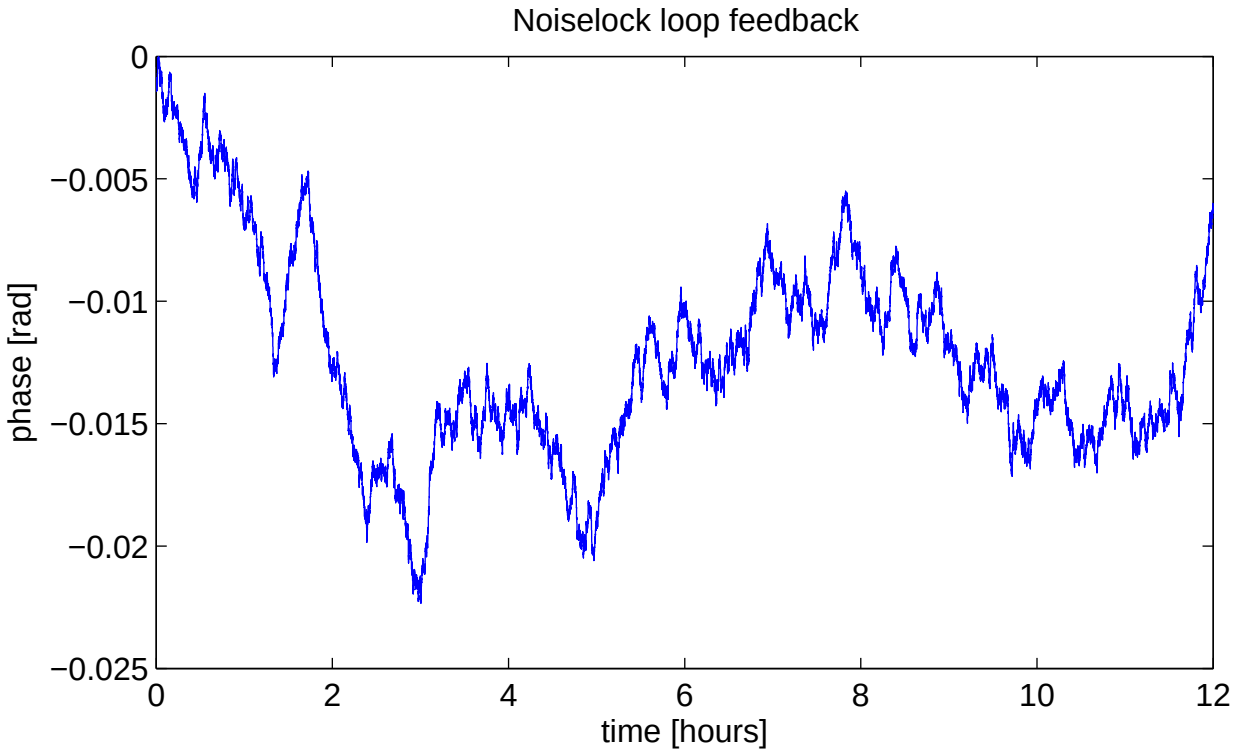

Figure 5: Example of drift of squeezer demodulation phase over the course of 12 hours.

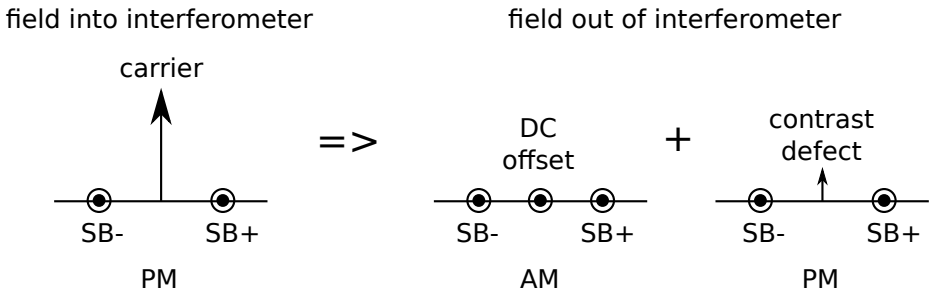

Figure 6: The RF sidebands (SB+ and SB-) are generated via phase modulation of the carrier field. The Michelson interferometer rotates the differential carrier field by 90°, but leaves all other fields the same, including the RF sidebands and the contrast defect. The result is that at the output port, the RF sidebands are amplitude modulation (AM) of the dark fringe offset, yet continue to be phase modulation (PM) of the contrast defect.

5.3 RF frequencies

This section is based on work from LIGO T0900325 and evaluates the role of the RF sidebands in generating phase jitter of the interferometer output field. Understanding the phase noise contribution from the RF sidebands is important both because the contribution can be large and because the squeezing ellipse orientation cannot follow at these frequencies. Phase noise due to the RF sidebands may, however, be reduced, as will be discussed shortly.

The dominant fields at the interferometer output port are those from the dark fringe offset, the contrast defect, and the RF sidebands. The dark fringe offset is the local oscillator for the gravitational-wave sidebands in a DC readout configuration and is generated by holding the Michelson arms slightly off of the dark fringe at the anti-symmetric port. The contrast defect is light that makes it to the anti-symmetric port due to asymmetry in the reflectivity of each Michelson arm. The RF sidebands are ideally filtered by the OMC, but due to limited finesse, some percentage is transmitted.

One of two effects of the RF sidebands on phase jitter comes from the fact that the Michelson interferometer rotates the differential carrier field by 90°, but leaves all other fields the same (including the RF sidebands and the contrast defect). The result is that at the output port, as shown in Figure 6, the RF sidebands are amplitude modulation (AM) of the dark fringe offset, yet continue to be phase modulation (PM) of the contrast defect.

Because the squeezing quadrature is determined by the sum of the fields at the interferometer output, both AM of the dark fringe offset and PM of the contrast defect affect the angle that the squeezing ellipse orientation must be matched to. Figure 7 shows phasors depicting these two situations. Should the ratio of dark fringe offset to contrast defect amplitude be large, these effects are reduced.

The second effect of the RF sidebands on phase jitter arises when the upper and lower sidebands are unequal in amplitude. Rather than produce pure AM on the DFO and PM on the CD, there is some component of PM on the DFO and AM on the CD.

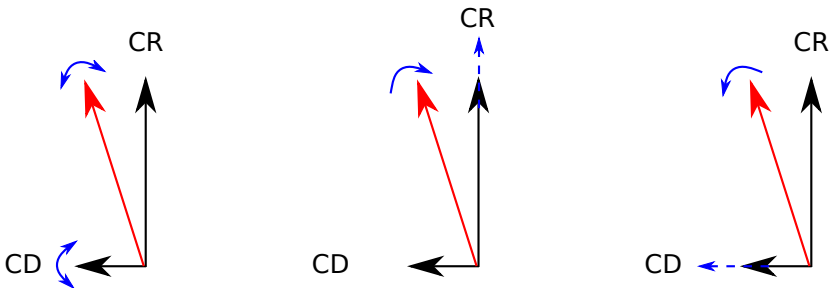

Figure 7: Examples of how jitter of the squeezing quadrature is generated. replace!

In summary, changes in the interferometer output phase at RF frequencies are created in four ways:

- phase noise of the contrast defect
- amplitude noise of the dark fringe offset
- phase noise of the dark fringe offset due to unequal RF sideband amplitudes
- amplitude noise of the contrast defect due to unequal RF sideband amplitudes (true?)

and may be expressed mathematically as in Eq. 90 from T0900325:

$$\Gamma_{\mathrm{rms}} = \sqrt{\frac{P_{\mathrm{SB}}}{P_{\mathrm{CR}}}\left(\frac{1}{\eta} + \epsilon^2 \frac{\eta - 1}{\eta}\right)} \tag{2}$$

All powers in this equation are for those transmitted through the OMC, and the variables η and ϵ are defined as follows:

$$\eta = \frac{P_{\mathrm{CR}}}{P_{\mathrm{CD}}} \tag{3}$$

$$\epsilon = \frac{1}{2}\frac{P_{\mathrm{SB+}} - P_{\mathrm{SB-}}}{P_{\mathrm{SB+}} + P_{\mathrm{SB-}}} \tag{4}$$

The sideband imbalance is quantified by ϵ and a sample measurement of the imbalance is shown in Figure 8a. Currently, $\epsilon = 0.06$. The contrast defect, commonly quoted as $1/\eta$, can be measured by comparing the power transmitted through the OMC with and without the dark fringe offset. It accounts for approximately 5% of the power at the output port, as seen in Figure 8b.

Figure 9 shows the dependence of phase noise on contrast defect for our current sideband imbalance. This uses $P_{CR} = 1.6$ and $P_{MI\_SB+} = 0.08 T_{MI}$ (for the 4.4× sideband amplitude reduction). We estimate the signal recycling cavity sideband amplitude as $P_{SR\_SB+} = 0.02 T_{SC}$. Note T_{MI} and T_{SR} are calculated in Table 1. We explored the affect of these factors on observed squeezing by changing the rms phase noise up to a factor of 4.4 by reducing the sideband amplitude. We also tried increasing the dark fringe offset. The result was ....

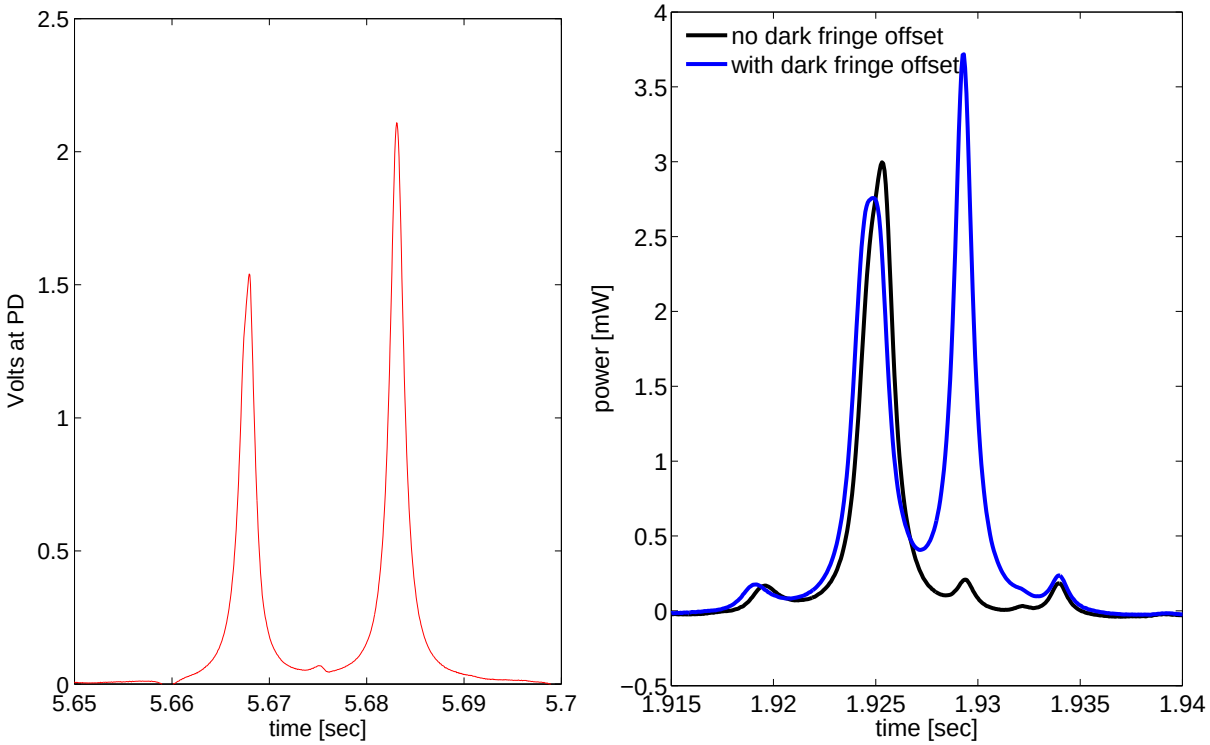

Figure 8: Mode scan of the output port. The left-hand plot shows the Michelson RF sideband imbalance. A higher-order carrier mode sits on top of the lower sideband, so this figure is created by subtracting the carrier content. The imbalance is $\epsilon = 0.06$. The right-hand plot shows the ratio of contrast defect to carrier power for our typical dark fringe offset. The ratio is about 0.05. The sideband amplitude reduced by a factor of 4.4 from fall 2011 and is the new standard.

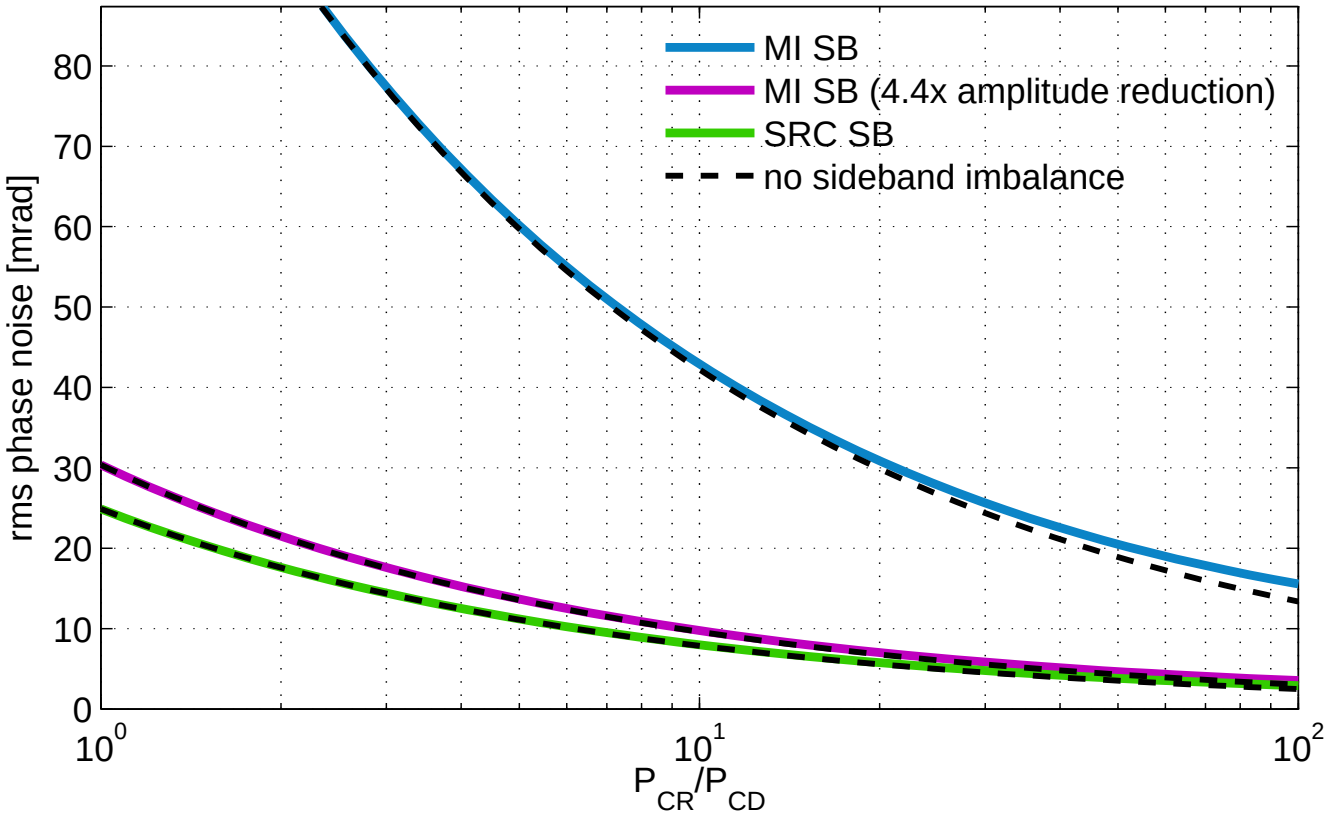

Figure 9: RMS phase noise as a function of the ratio of DC offset light to contrast defect light in the OMC transmitted beam. The typical operating point for GEO is $P_{\rm CR}/P_{\rm CD} = 20$, which corresponds to an RMS phase noise for the Michelson sidebands of 6.7 mrad and 5.5 mrad for the SRC sidebands. The quadrature sum is 8.7 mrad.

Table 3: Measured and calculated phase noises. The quadrature sum is 10 mrad rms.

source	rms phase [mrad]
error point	5
14.9 MHz sidebands	6.7
9 MHz sidebands	5.5

5.4 Higher order modes

Role?

5.5 Total known phase noise

Taking the measured and anticipated rms phase noises at different frequencies and adding them incoherently, we find that we have a total known phase noise of 10 mrad rms. The summary of phase noises is shown in Table 3.

6 Expected observed squeezing

Based on our measurements of the optical losses and phase noise, we can predict the best possible achieveable squeezing level with the interferometer output. With a green pump power of about 17 mW such that the injected squeezing level is 8 dB and 37% losses, the best squeezing possible is 3.2 dB. Phase noise of 10 mrad has a negligible effect. As of early March, we measured 2.9 dB, leaving a 0.3 dB gap, which in fact is explained by other contributing noise sources as seen in the next section. This full accounting of observed squeezing is not always realized, however. Currently, as of mid-April, for example, there remains a gap.

7 Other noise sources

Other noise sources like dark noise and laser amplitude noise limit the amount of detected squeezing. Figure 10 ...

8 Ideas for improvements

1. better OMC

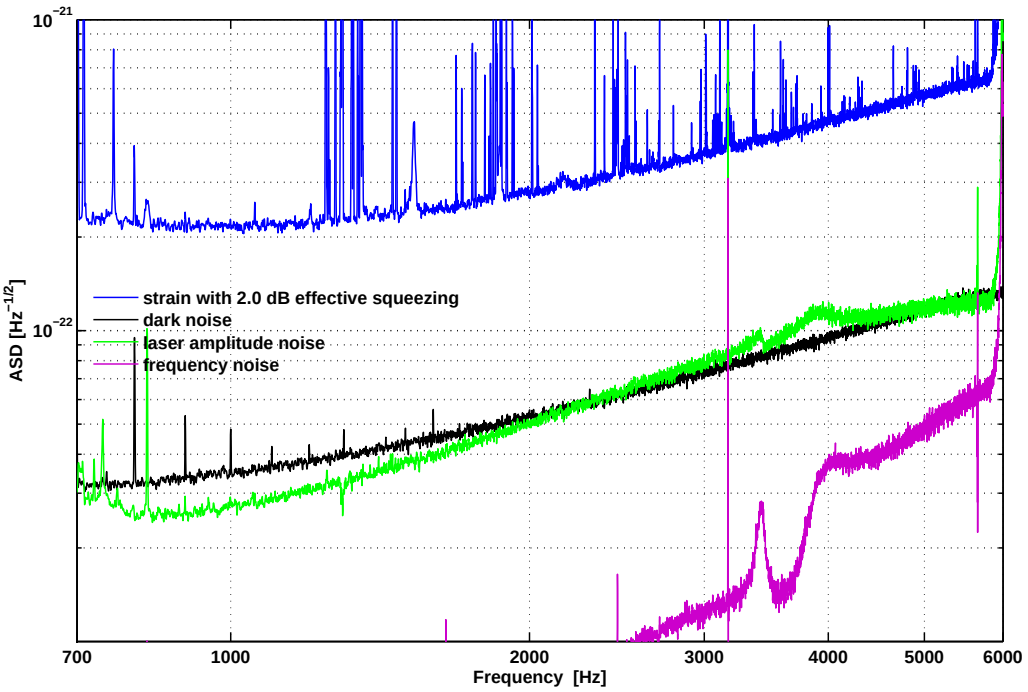

Figure 10: High frequency noises that result in a lower effective squeezing of strain than is actually achieved. In this example, shot noise is actually reduced by 2.4 dB, but the other noise sources reduce the effective squeezing to 2.0 dB.

Table 4: Optical losses of squeezed beam.

component	power loss	6-month goal
squeezer path Faraday	3.3%	1.5%
output port Faraday	3.3% × 2	1.5% × 2
BDO1 transmission	1% × 2	1% × 2
SR cavity (when locked)	1%	1%
OMC mode-matching loss	6%	2%
squeezer mode-matching loss	2%	2%
OMC AR coating loss	1%	0.1%
OMC internal losses	14%	5%
OMC trans PD detection loss	9%	3%

2. 2 PDs
3. 2nd OMC

9 Acknowledgements